Integration of Hydrogen in Sequential Monte Carlo Power Systems Adequacy Assessment

Aurélia Hernandez
Institute of Mechatronic, Electrical Energy, and Dynamic Systems, UCLouvain
Louvain-la-Neuve, Belgium
aurelia.hernandez@uclouvain.be

François Vallée
Power Systems and Markets Research Group, UMons
Mons, Belgium
francois.vallee@umons.ac.be

Emmanuel De Jaeger
Institute of Mechatronic, Electrical Energy, and Dynamic Systems, UCLouvain
Louvain-la-Neuve, Belgium
emmanuel.dejaeger@uclouvain.be

***Abstract*—Green hydrogen, i.e. hydrogen produced by low-carbon energy sources is a popular candidate for decarbonizing the energy sector. Used as a feedstock, a fuel, or a storage medium, it is most likely to be part of the future energy system. For this reason, hydrogen is the subject of numerous studies. However, its impact on the adequacy of power systems has not been fully studied. This work aims to integrate the hydrogen energy vector within a sequential Monte Carlo adequacy tool based on a multi-period DC optimal power flow tailored for long time horizons (e.g. one year). The proposed study takes into account the hydrogen energy vector by integrating a hydrogen system composed of an electrolyzer, a hydrogen-to-power unit, and a hydrogen storage, in a test system. The obtained results allow to grasp insights on the effect that hydrogen storage, hydrogen demand, and hydrogen imports can have on power system adequacy.**

***Index Terms*—Adequacy, electrolyzers, hydrogen, multi-period DC optimal power flow, sequential Monte Carlo simulations.**

I. Introduction

In recent years, Europe has set some targets for the energy transition: reduction of 55% of GHG emissions compared to 1990 level (Fit-for-55 Package) by 2030 and carbon neutrality by 2050. As the energy sector represents more than 75% of the european GHG emissions [1], the decarbonation of this sector is thus necessary and essential to reach the aforementioned objectives. In this context, green hydrogen, i.e. hydrogen produced from water electrolysis fed by low carbon energy sources, could help decarbonize the mobility and industry sectors - which are hard-to-decarbonize sectors because part of their applications cannot be electrified - and the power sector. In addition to being a feedstock and a potential fuel for conversion technologies, hydrogen can also be stored under the form of molecules. For these reasons, many studies assert that hydrogen will be part of future energy systems. Several technologies, such as electrolyzers and hydrogen-to-power units, link the hydrogen sector and electrical power systems. For this reason, it is relevant to integrate hydrogen into power system studies, and especially adequacy studies. Indeed, with the increase in renewable energies, it has become crucial to asses the adequacy of power systems through probabilistic adequacy studies.

Hydrogen has been considered in power system operation by several authors already. The dynamic and reactive behaviour of electrolyzers is integrated into a security-constrained multi-period AC optimal power flow (SC-MP-AC-OPF) in [2]. Energy hubs consisting in electrolyzers, hydrogen storage, and hydrogen-to-power units, are integrated into a three stage robust security-constrained multi-period unit commitment DC power flow (SC-MP-UC-DC-PF) in [3]. Hydrogen storage is considered in a stochastic SC-UC-DC-OPF in [4]. All these studies optimize the operational costs on a daily basis. Hydrogen is also integrated into a multi-energy UC-DC-OPF model which optimizes both the annuitized investment and operation costs in [5]. Hydrogen is integrated into a multi-energy model framework REMix in [6] which optimizes both operational and investment costs and focuses on the hydrogen infrastructure expansion.

Also, many studies have assessed the reliability of integrated gas-power systems. Their reliability is assessed in an event-based non-sequential sampling in [7,8], in a 2 hours time horizon in [9], in a daily time horizon in [10]–[13], in a weekly time horizon in [14], in a yearly time horizon in [15]–[17], and on a several year time horizon considering investment costs in [18]. Usually, the main objective is to model precisely the availability of gas-fired units which play a major and growing role in power systems. Although all studies consider gas-fired units as the technologies that link both systems, few studies [7,10,15,18] also consider power-to-gas technologies allowing bi-directional flows between both systems.

Literature on the impact of hydrogen on the system's adequacy has been studied by two authors. Firstly, the impact of producing hydrogen and storing it to manage over-production of wind power sources from a market-based point of view was studied within a sequential Monte Carlo adequacy framework in [19]. This study does not consider network constraints. Secondly, the fraction of blended hydrogen was considered in gas flow equations and the effects on integrated gas-power systems reliability were studied in [20]. Hydrogen demand is considered in the first study, while hydrogen-to-power units are not considered in either studies.

To the author's knowledge, no study spotlights the impact of hydrogen in terms of demand, storage and imports on power system adequacy studies. This work therefore aims at fulfilling this gap. The main contributions of this work are:

i) The development of a novel sequential Monte Carlo tool

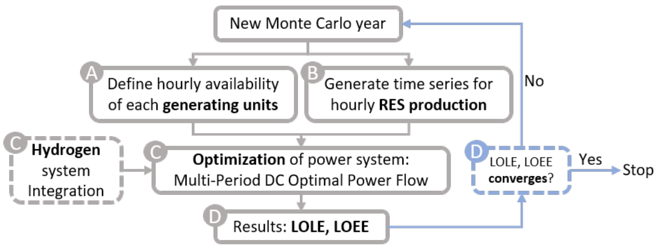

Fig. 1. Implemented Sequential Monte Carlo Process.

for adequacy studies based on a multi-period DC optimal power flow (MP-DC-OPF) with an hourly resolution and specifically tailored for long time horizons, e.g. 1 year.

ii) The integration of the hydrogen energy vector within the MP-DC-OPF with its conversion and storage technologies (electrolyzers, hydrogen-to-power units, hydrogen storage units).

iii) The study of the impact of hydrogen on adequacy and on the operation of a modified test system representative of future transmission grids.

The work presented in this paper is structured according to the following sections: Section II resumes the sequential Monte Carlo process used to assess the adequacy. Section III describes the case study. Section IV presents and analyses results for different scenarios, and Section V concludes the work of this paper.

II. Methodology

Sequential Monte Carlo (MC) simulations are used to assess the adequacy of power systems. They are preferred rather than analytical methods as they can be applied to more complex systems while keeping reasonable computational time. Moreover, sequentiality is chosen in order to consider seasonality. The MC process is depicted in Fig. 1. For each MC year, the availability of the generating units are defined (section II-A), as well as the renewable power potential (section II-B). These time series will be used to perform a DC-OPF (section II-C), the results of which will be used to extract the adequacy indicators (section II-D).

A. Availability of Conventional Generating Units

The availability of conventional generating units is represented using a two-state Markov model. For each MC year, the yearly availability profile of each unit is determined by random sample draws from the time-to-failure TTF and time-to-repair TTR distributions. TTF and TTR have negative exponential distributions characterized by $MTTF$ and $MTTR$, their mean-TTF and mean-TTR respectively.

B. Capacity Factor of Wind Power

For each MC year, an hourly profile is generated thanks to an auto-regressive and moving average (ARMA) model which is built based on historical data.

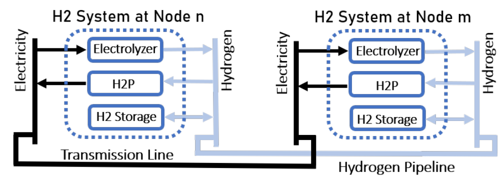

Fig. 2. Hydrogen System Representation.

C. Multi-Period DC Optimal Power Flow (MP-DC-OPF)

Hydrogen systems (see Fig. 2) composed of electrolyzers, hydrogen storage units, and hydrogen-to-power units are integrated into the MP-DC-OPF. In this formulation, Variables are denoted with an upper case letter as first letter, and parameters with a lower case letter.

1) Objective function: The costs related to the operation of the conventional generating units, the energy-not-served, the operation of electrolyzers, and the hydrogen imports are minimised and detailed in (1).

$$\text{Min} \sum_{t=1}^{8760} \left(\sum_{g=1}^{n_g} c_{gen}(g) \cdot P_{gen}(g,t) + \sum_{n=1}^{n_n} voll \cdot Ens(n,t) \right.$$
$$\left. + c_{el} \cdot P_{el}(n,t) + c_{H_2} \cdot Q_{H_2,imp}(n,t) \right) \qquad (1)$$

With $c_{gen}(g)$, c_{el}, and c_{H2} the costs [€/MWh] of generator g, electrolyzer operation, and hydrogen imports respectively, $voll$ [€/MWh] the value of loss-load, $P_{gen}(g,t)$ the hourly production [MWh/h] of conventional generator g, $P_{el}(n,t)$ the hourly consumption [MWh/h] of electrolyzer at node n, and $Q_{H2,imp}(n,t)$ [MWh/h] the hydrogen imports at node n.

2) Electrical balance: At each hour t of the year and at each node n of the system, electrical energy has to comply with the conservation of energy. The power produced by the conventional generators, and the renewable sources has to satisfy the electrical load with the integration of a hydrogen system. If unbalances occur, production is curtailed (excess) or energy is not served (lack).

$$\sum_{g \in G_n} P_{gen}(g,t) + \sum_{r \in R_n} res(r,t) + P_{H2P}(n,t)$$
$$+ \sum_{k \in L_{to,n}} F(k,t) - \sum_{k \in L_{from,n}} F(k,t) = d_l(n) \cdot l(t) +$$
$$(1+\eta_c) \cdot P_{el}(n,t) - Ens(n,t) + C(n,t) \quad \forall n, \forall t \qquad (2)$$

With $d_l(n)$ the nodal load distribution, $l(t)$ the hourly load [MWh/h], η_c the part of electrolyzer consumption dedicated to compression needs, $res(r,t)$ the hourly energy produced [MWh/h] by renewable energy source r, $P_{H2P}(n,t)$ the hourly energy produced [MWh/h] by H2P units at node n, $F(k,t)$ the hourly energy [MWh/h] flowing through line k, and $C(n,t)$ the hourly curtailment at node n .

3) Conventional Generators: Production of conventional generators is limited by their maximum power capacity $p_{conv,max}(g)$ [MW], and by their availability $\alpha_{gen}(g,t) \in [0;1]$ at each time step. The unavailabilities represent unplanned forced outages.

$$P_{gen}(g,t) \leq \alpha_{gen}(g,t) \cdot p_{gen,max}(g) \qquad \forall g, \forall t \quad (3)$$

4) Power Load Flow: A DC load flow is used to model the power flows within the network.

$$F(k,t) = u_b^2 \cdot b(k) \cdot (\Theta(n_{fr,k},t) - \Theta(n_{to,k},t)) \quad \forall k, \forall t \quad (4)$$
$$\Theta(n_{ref},t) = 0 \qquad \forall t \quad (5)$$

With u_b the voltage [kV], $b(k)$ the susceptance [S] of the line k, $\theta(n,t)$ the hourly phase angle of node n, and $n_{from}(k)$ and n_{to}(k) the two nodes bounding line k. These flows are limited by the maximum capacity of the lines $f_{max}(k)$ [MW].

$$-f_{max}(k) \leq F(k,t) \leq f_{max}(k) \qquad \forall k, \forall t \quad (6)$$

5) Electrolyzers: Hydrogen can be produced through electrolyzers and their installed capacity $p_{el,max}(n)$ [MW] limits their power operation.

$$P_{el}(n,t) \leq p_{el,max}(n) \qquad \forall n, \forall t \quad (7)$$

6) Hydrogen-to-Power units: These units convert hydrogen into electrical power and their operation are limited by their installed capacity $p_{H2P,max}(n)$ [MW].

$$P_{H2P}(n,t) \leq p_{H2P,max}(n) \qquad \forall n, \forall t \quad (8)$$

7) Hydrogen balance constraint: Hydrogen also has to comply with the conservation of energy. Hydrogen produced by electrolyzers with an efficiency η_{el}, and imported has to feed the hydrogen demand, and the H2P units with the support of hydrogen storage. The H2P units produce electricity with a certain efficiency η_{H2P}.

$$\begin{aligned} &P_{el}(n,t) \cdot \eta_{el} + Q_{H_2,sto,out}(n,t) + Q_{H_2,imp}(n,t) \\ &+ \sum_{j \in PL_{to,n}} F_{H_2}(j,t) - \sum_{j \in PL_{from,n}} F_{H_2}(j,t) = Q_{H_2,dem}(n,t) \\ &+ Q_{H_2,sto,in}(n,t) + \frac{P_{H2P}(n,t)}{\eta_{H2P}} \qquad \forall n \end{aligned} \quad (9)$$

With $Q_{H_2,sto,in/out}(n,t)$ the hourly input/output flows [MWh/h] of the hydrogen storage at node n, $F_{H_2}(j,t)$ the hourly hydrogen [MWh/h] flowing through pipeline j, and $Q_{H_2,dem}(n,t)$ the hourly hydrogen production [MWh/h] dedicated to the exogenous hydrogen demand.

8) Hydrogen Pipelines: Hydrogen can be transported through pipelines. This transported quantity is limited by the maximum transfer capacity $f_{H_2,max}(j)$ [MW] of the latter.

$$-f_{H_2,max}(j) \leq F_{H_2}(j,t) \leq f_{H_2,max}(j) \qquad \forall j, \forall t \quad (10)$$

9) Hydrogen storage management: Hydrogen can be stored under the form of compressed gas. The storage is assumed to be empty at the beginning of the year. The hourly state-of-charge $Soc_{H_2,sto}(n,t)$ [MWh] is updated at each time step and for each node n in (13) and is limited by its maximum capacity $soc_{H_2,sto,max}(n)$ [MWh] in (14).

$$Soc_{H_2,sto}(n,t=1) = Q_{H_2,sto,in}(n,t=1) \qquad \forall n \quad (11)$$
$$Q_{H_2,sto,out}(n,t=1) = 0 \qquad \forall n \quad (12)$$
$$\begin{aligned} Soc_{H_2,sto}(n,t) &= Soc_{H_2,sto}(n,t-1) + Q_{H_2,sto,in}(n,t) \\ &- Q_{H_2,sto,out}(n,t) \quad \forall n, \forall t > 1 \end{aligned} \quad (13)$$
$$Soc_{H_2,sto}(n,t) \leq soc_{H_2,sto,max}(n) \qquad \forall n, \forall t \quad (14)$$

10) Hydrogen Demand: The hydrogen demand can be flexible or non-flexible. In (15), no flexibility is permitted and the formulation constrains the hourly hydrogen production to equal at each node a certain percentage $d_{H2}(n)$ of the hourly exogenous hydrogen demand $q_{H2,exo}(t)$ [MWh/h]. In (16), a yearly flexibility allows the annual hydrogen demand to be produced optimally whenever during the year. These constraints are exclusive and cannot be implemented together.

$$Q_{H_2,dem}(n,t) = d_{H_2}(n) \cdot q_{H_2,exo}(t) \qquad \forall n, \forall t \quad (15)$$
$$\sum_{t=1}^{8760} Q_{H_2,dem}(n,t) = d_{H_2}(n) \cdot \sum_{t=1}^{8760} q_{H_2,exo}(t) \qquad \forall n \quad (16)$$

D. Adequacy indicators and Convergence

The loss-of-load LOL_y [hours/year] and loss-of-energy LOE_y [MWh/year] expressed in (17) and (18) are calculated for each MC year and the adequacy indicators LOLE and LOEE, i.e. the LOL- and LOE-expectations expressed in (17) and (18), are derived for each simulation. In (17) and (18), c_t is a boolean variable that equals 1 if energy is not served at hour t and 0 if not, $Ens(n,t)$ is the energy-not-served [MWh/h] at node n and hour t, and n_{mc} is the number of MC years in a simulation which depends on the convergence indicator in (19).

$$LOL_y = \sum_{t=1}^{8760} c_t \rightarrow LOLE = \frac{\sum_{y=1}^{n_{mc}} LOL_y}{n_{mc}} \quad (17)$$
$$LOE_y = \sum_{t=1}^{8760} \sum_{n=1}^{n_n} Ens(n,t) \rightarrow LOEE = \frac{\sum_{y=1}^{n_{mc}} LOE_y}{n_{mc}} \quad (18)$$

$$\epsilon = \frac{\sigma(X)}{\sqrt{n_{mc}} E(X)} \leq \epsilon_{threshold} \quad (19)$$

Where X represents the LOLE and LOEE respectively. The threshold is set to $\epsilon_{threshold} = 0.03$ in this study.

III. Case Study

The previously described methodology is applied to the Roy Billinton Test System (RBTS) [21] which is modified to represent future transmission power systems, i.e. high offshore wind penetration level located at the outskirts of the system, with one remote hydrogen system located near the renewable energy source, and another centered near the consumers. The system originally consists in 6 buses, 9 lines, a 185 MW peak load, and 11 generators (thermal and hydro) located at Bus 1 and 2 respectively with a total capacity of 240 MW. This test

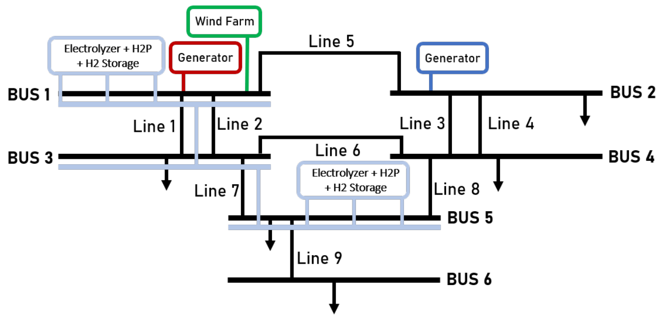

Fig. 3. Modified Roy Billinton Test System.

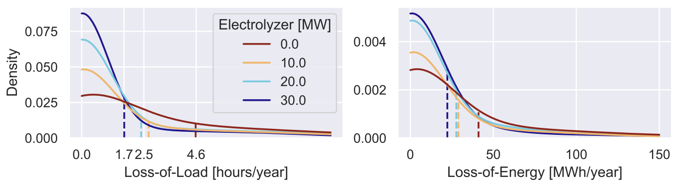

Fig. 4. Kernel Distribution Estimate (KDE) of the LOL and LOE for every electrolyzer capacity - Scenario 1.

system is modified (see Fig. 3) by removing a 40 MW thermal unit at Bus 1, adding a wind farm (WF) at Bus 1, a hydrogen system at Buses 1 and 5, and a hydrogen pipeline linking both hydrogen assets. Different sizes of hydrogen systems will be tested, but it will always follow the following configuration:

$$p_{H2P,max}(n) = p_{el,max}(n) \qquad \forall n$$
$$soc_{H_2,sto,max}(n) = Ratio \cdot p_{el,max}(n) \qquad \forall n$$

with $Ratio$ refering to the hydrogen storage ratio. The efficiency of the electrolyzers and H2P units are set to $\eta_{el} = 0.7$ and $\eta_{H2P} = 0.43$ respectively. These values are taken arbitrarly from ranges proposed by [22]. The hydrogen pipelines are assumed to have a 100 MW maximum capacity.

IV. Results

A. Scenario 1: RBTS with 100 MW Wind Farm, H_2 Sto. Ratio 3, No H_2 Demand, No H_2 Imports.

The empirical probability distribution function of the Loss-of-Load is plotted in Fig. 4. There is a clear correlation between the hydrogen system size and the LOLE (see vertical line projected on x-axis). When installing 10 MW (2x5 MW: 5 MW at Bus 1 and 5 MW at Bus 5) of electrolyzers, the LOLE decreases by 41%, and when reaching 20 (2x10 MW) and 30 MW (2x15 MW), it decreases by 48% and 63% respectively. For the sake of clarity, the x-axis has been cut and the figure does not show extreme cases that can reach high values of LOL and LOE. The same analysis can be made for the LOEE in Fig. 4. It decreases by 29.5, 32.5 and 46% when installing 10, 20 and 30 MW of electrolyzers respectively.

These results can be put into perspective by observing outputs other than the adequacy indicators. The yearly curtailment (see Fig. 5) decreases when the hydrogen system capacity increases. Initially around 5 GWh/year, it decreases by 46, 70, and 82% when installing 10, 20, and 30 MW of electrolyzers respectively.

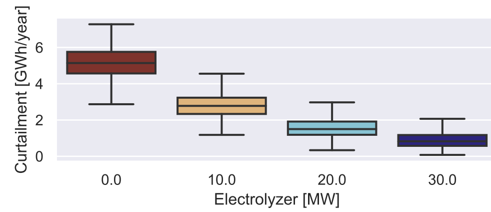

Fig. 5. Distribution of the yearly curtailment for every electrolyzer capacity - Scenario 1.

TABLE I
Evolution of the capacity and load factors [%] of the hydrogen assets when increasing the electrolyzers installed - Scenario 1.

H2 Technology	2x5 MW	2x10 MW	2x15 MW
Electrolyzer Node 1	7.5	6.5	5.8
Electrolyzer Node 5	7.17	5.89	5.06
H2P Node 1	2.52	2.24	2.04
H2P Node 5	1.89	1.5	1.59

The yearly production of generators increase slightly when adding hydrogen storage systems. Indeed, it increases by 1% when adding 30 MW of electrolyzers. This is due to the system trying to reduce its cost by increasing and storing cheap hydro power in order to use it instead of expensive thermal power plants when hydro plants are already at their maximum production. However, going through the hydrogen storage system leads to additional losses (round-trip efficiency of 30%), so this strategy increases the overall production of conventional generators.

The yearly resume of the operation of hydrogen assets, i.e. the energy consumed and produced by electrolyzers and H2P plants, as well as the number of equivalent cycles in the hydrogen storage facility defined as:

$$\text{Eq. Nb. Cycles } (n) = \frac{\sum_{t=1}^{8760} Q_{h2,sto,in}(n,t)}{soc_{max}(n)} \tag{20}$$

are illustrated in Fig. 6. Firstly, electrolyzers and H2P consume/produce more when the installed capacity of electrolyzers and H2P increases (Fig. 6: top-mid row). However it should be put into perspective with the evolution of their respective utilisation factor. Indeed, the load and capacity factor of the latter can be found in Table I. They decrease when the installed capacity increases. Secondly, the equivalent number of cycles of the hydrogen storage (Fig. 6: bottom row) gives an insight on the utilisation of the hydrogen storage. In this scenario, the mean value lies between 412 and 428 equivalent cycles. When increasing the electrolyzer capacity, the values decrease a bit due to the fact that the load factor of electrolyzers decreases as well.

B. Sensitivity analysis of Scenario 1: Wind Farm capacity and H_2 Sto. Ratio variations for different Hydrogen System Size.

Two scenarios (WF = 100 and 200 MW) with their variants (H_2 Sto. Ratio = 2,3,6) are compared and studied in this

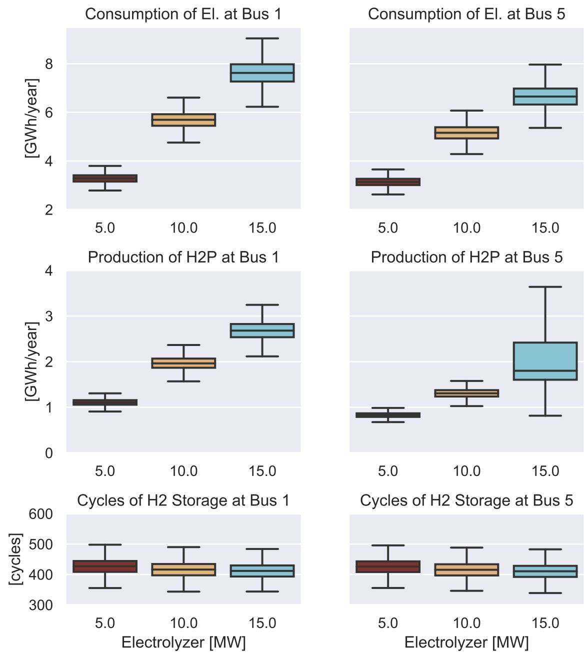

Fig. 6. Distribution of energy consumption/production of the hydrogen assets for every electrolyzer capacity. Top row: Electrolyzers at Node 1 and 5. Mid row: H2P at Node 1 and 5. Bottom row: Equivalent number of cycles of the H2 storage - Scenario 1.

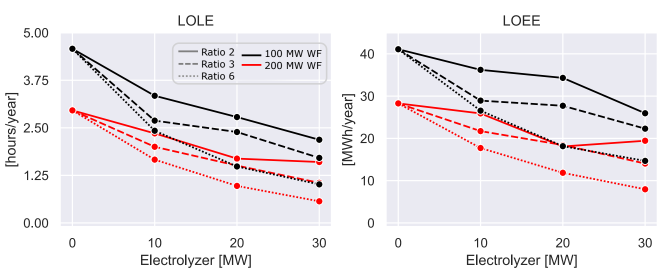

Fig. 7. LOLE and LOEE evolution when increasing the electrolyzer capacity size for different scenarios - Scenario 1.

section. Their adequacy results (LOLE and LOEE) are plotted and compared in Fig. 7. Firstly, the hydrogen system size, the hydrogen storage ratio, and the wind penetration level are favourable to the adequacy of the system. Secondly, these positive effects overlap at some point. Indeed, when 10 MW of electrolyzers are installed, having a 100 MW or a 200 MW wind farm can be equivalent in terms of adequacy if the hydrogen storage is increased by a factor 3, i.e. from 20 MWh (Ratio 2), to 60 MWh (Ratio 6). The same analysis is made when 20 MW of electrolyzers are installed, having a 100 MW or a 200 MW wind farm can be equivalent in terms of adequacy if the hydrogen storage is increased by a factor 2, i.e. from 60 MWh (Ratio 3), to 60 MWh (Ratio 6). Moreover, above 20 MW of electrolyzers installation, the test system with a 100 MW wind farm can be more reliable than with a 200 MW wind farm for a certain hydrogen storage capacity.

C. Scenario 2: 300 MW Wind Farm, Varying Hydrogen System, With Hydrogen Demand, No H_2 Sto.

The integration of a hydrogen demand is studied in this section. Two cases are compared: a yearly flexible vs. a non-flexible hydrogen demand and the adequacy results are

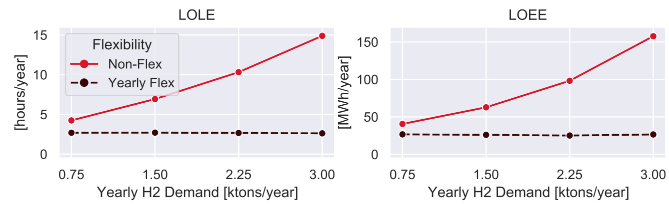

Fig. 8. LOLE and LOEE evolution when increasing the yearly hydrogen demand - Scenario 2.

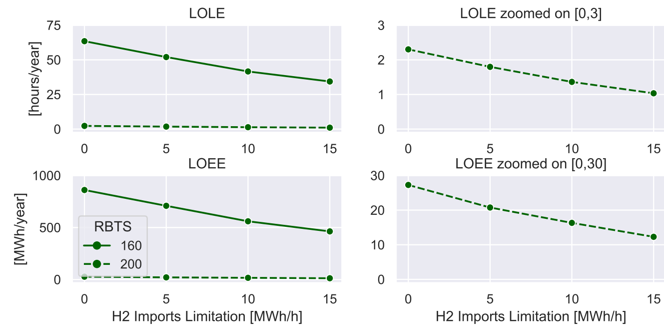

Fig. 9. LOLE and LOEE evolution when increasing the hydrogen importation limit - Scenario 3.

plotted in Fig. 8. For each hydrogen demand (0.75-1.5-2.25-3 kt/year), a different electrolyzer capacity (30-60-90-120 MW) is installed to satisfy this demand. The flexible case is almost not impacted by the integration of a hydrogen demand, while the non-flexible case increases its LOLE and LOEE by a factor 6 and 6.7 respetively when integrating a yearly demand of 3 ktons of hydrogen.

D. Scenario 3: 100 MW Wind Farm, H_2 Sto. Ratio 3, 10 MW Electrolyzers, No H_2 Demand, With H_2 Imports.

In this section, hydrogen imports are permitted and integrated into the test system. Two cases are compared: the modified RBTS with 200 MW vs. 160 MW (removal of an extra 40 MW thermal unit) of conventional power units. Firstly, it can be observed in Fig. 9 that for both cases, allowing hydrogen imports enhances adequacy. The LOLE and LOEE can be reduced up to 46 and 55% for RBTS 160 and RBTS 200 MW respectively when allowing 15 MWh/h of hydrogen imports. Secondly, the distribution of the yearly hydrogen imports for the different cases is depicted in Fig. 10. Their is an order of magnitude between both cases. Indeed, RBTS 200 MW is already highly reliable (LOLE $\sim$ 2.5 hours) and thus only imports when lacking energy which is rare while the case RBTS 160 MW is not reliable (LOLE $\sim$ 65 hours) and thus imports much more hydrogen to produce electricity with the H2P units.

V. Conclusion

This paper presents the impact that hydrogen can have on power system adequacy assessments. To do so, a novel sequential Monte Carlo adequacy tool based on a multi-period DC optimal power flow model is developed. In this model, the hydrogen energy carrier is integrated, as well as the assets

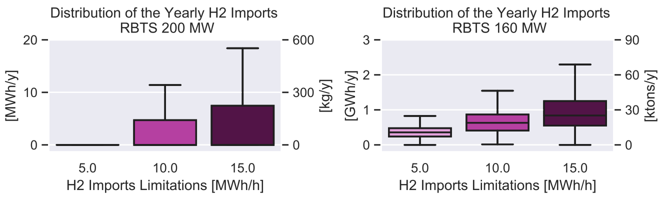

Fig. 10. Distribution of the yearly H2 imports - Scenario 3.

that link hydrogen to the power system, i.e. electrolyzers, and hydrogen-to-power units, and hydrogen storage units.

The methodology is applied to a modified Roy Billinton Test System and different scenarios are analysed.

The first scenario highlighted the positive effect of different hydrogen system assets on the systems adequacy and operation: hydrogen systems with a power capacity of 10-20-30 MW and a hydrogen storage of 30-60-90 MWh could reduce the LOLE by 41-48-63 % and the LOEE by 29.5-32.5-46 % respectively, and reduce the curtailment by 46-70-82 %. The results also showed that though consumption/production of electricity from electrolyzers, and H2P units increase with the capacity installed, their respective load/capacity factor decreases. Moreover, the effect of wind farm capacity, hydrogen storage ratio, and hydrogen system size was also analysed. This sensitivity analysis underlines the importance of a compromise between different installed capacity of the assets and highlights the relevance of optimising these capacities in further studies.

The second scenario analysed the effect of introducing a certain hydrogen demand, and showed that allowing some flexibility can help the system cope with this additional indirect electrical demand.

The third scenario integrated hydrogen imports. It is clearly beneficial for the power system and especially if the system does not have sufficient conventional generators, and relies on hydrogen-to-power units and hydrogen imports.

Future works will i) apply the methodology to a congested network to see if hydrogen transport is a realistic candidate for stressed networks, ii) apply the methodology to a more complex and realistic system, iii) introduce outages for the transmission lines, pipelines, and hydrogen assets.

VI. Acknowledgements

This research is supported by the Energy Transition Funds project “BEST” organized by the Belgian FPS economy.

References

[1] EC, “Énergie et pacte vert pour l’europe,” Available at https://ec.europa.eu/info/strategy/priorities-2019-2024/european-green-deal/energy-and-green-deal_fr, (5/12/22).

[2] A. Rabiee, A. Keane, and A. Soroudi, “Green hydrogen: A new flexibility source for security constrained scheduling of power systems with renewable energies,” *International Journal of Hydrogen Energy*, vol. 46, no. 37, pp. 19 270–19 284, May 2021.

[3] M. Ban, J. YU, M. Shahidehpour, and Y. YAO, “Integration of power-to-hydrogen in day-ahead security-constrained unit commitment with high wind penetration,” *Journal of Modern Power Systems and Clean Energy*, vol. 5, Apr. 2017.

[4] M. A. Mirzaei, A. Sadeghi Yazdankhah, and B. Mohammadi-Ivatloo, “Stochastic security-constrained operation of wind and hydrogen energy storage systems integrated with price-based demand response,” *International Journal of Hydrogen Energy*, vol. 44, no. 27, pp. 14 217–14 227, May 2019.

[5] P. Fu, D. Pudjianto, X. Zhang, and G. Strbac, “Integration of Hydrogen into Multi-Energy Systems Optimisation,” *Energies*, vol. 13, no. 7, p. 1606, Jan. 2020.

[6] H. C. Gils, H. Gardian, and J. Schmugge, “Interaction of hydrogen infrastructures with other sector coupling options towards a zero-emission energy system in Germany,” *Renewable Energy*, vol. 180, pp. 140–156, Dec. 2021.

[7] C. Wang, H. Xie, Z. Bie, G. Li, and C. Yan, “Fast supply reliability evaluation of integrated power-gas system based on stochastic capacity network model and importance sampling,” *Reliability Engineering & System Safety*, vol. 208, p. 107452, Apr. 2021.

[8] A. Antenucci and G. Sansavini, “Adequacy and security analysis of interdependent electric and gas networks,” *Proceedings of the Institution of Mechanical Engineers, Part O: Journal of Risk and Reliability*, vol. 232, no. 2, pp. 121–139, Apr. 2018.

[9] O. A. Ansari, C. Y. Chung, and E. Zio, “A Novel Framework for the Operational Reliability Evaluation of Integrated Electric Power–Gas Networks,” *IEEE Transactions on Smart Grid*, vol. 12, no. 5, pp. 3901–3913, Sep. 2021.

[10] S. Wang, Y. Ding, C. Ye, C. Wan, and Y. Mo, “Reliability evaluation of integrated electricity–gas system utilizing network equivalent and integrated optimal power flow techniques,” *Journal of Modern Power Systems and Clean Energy*, vol. 7, no. 6, pp. 1523–1535, Nov. 2019.

[11] M. A. Mirzaei, A. S. Yazdankhah, B. Mohammadi-Ivatloo, M. Marzband, M. Shafie-khah, and J. P. S. Catalão, “Stochastic network-constrained co-optimization of energy and reserve products in renewable energy integrated power and gas networks with energy storage system,” *Journal of Cleaner Production*, vol. 223, pp. 747–758, Jun. 2019.

[12] C. Juanwei, Y. Tao, X. Yue, C. Xiaohua, Y. Bo, and Z. Baomin, “Fast analytical method for reliability evaluation of electricity-gas integrated energy system considering dispatch strategies,” *Applied Energy*, vol. 242, pp. 260–272, May 2019.

[13] C. M. Correa-Posada and P. Sánchez-Martín, “Integrated Power and Natural Gas Model for Energy Adequacy in Short-Term Operation,” *IEEE Transactions on Power Systems*, vol. 30, no. 6, pp. 3347–3355, Nov. 2015.

[14] M. Chaudry, J. Wu, and N. Jenkins, “A sequential Monte Carlo model of the combined GB gas and electricity network,” *Energy Policy*, vol. 62, pp. 473–483, Nov. 2013.

[15] Z. Meng, S. Wang, Q. Zhao, Z. Zheng, and L. Feng, “Reliability evaluation of electricity-gas-heat multi-energy consumption based on user experience,” *International Journal of Electrical Power & Energy Systems*, vol. 130, p. 106926, Sep. 2021.

[16] H. Yang, Y. Zhang, Y. Ma, D. Zhang, L. Sun, and S. Xia, “Reliability assessment of integrated energy system considering the uncertainty of natural gas pipeline network system,” *IET Generation, Transmission & Distribution*, vol. 13, no. 22, pp. 5033–5041, 2019.

[17] X. Zhang, L. Che, M. Shahidehpour, A. S. Alabdulwahab, and A. Abusorrah, “Reliability-Based Optimal Planning of Electricity and Natural Gas Interconnections for Multiple Energy Hubs,” *IEEE Transactions on Smart Grid*, vol. 8, no. 4, pp. 1658–1667, Jul. 2017.

[18] C. He, L. Wu, T. Liu, and Z. Bie, “Robust Co-Optimization Planning of Interdependent Electricity and Natural Gas Systems With a Joint N-1 and Probabilistic Reliability Criterion,” *IEEE Transactions on Power Systems*, vol. 33, no. 2, pp. 2140–2154, Mar. 2018.

[19] P. Pelacchi and D. Poli, “The influence of wind generation on power system reliability and the possible use of hydrogen storages,” *Electric Power Systems Research*, vol. 80, no. 3, pp. 249–255, Mar. 2010.

[20] T. Wu and J. Wang, “Reliability Evaluation for Integrated Electricity-Gas Systems Considering Hydrogen,” *IEEE Transactions on Sustainable Energy*, pp. 1–14, 2022, in press.

[21] R. Billinton, S. Kumar, N. Chowdhury, K. Chu, K. Debnath, L. Goel, E. Khan, P. Kos, G. Nourbakhsh, and J. Oteng-Adjei, “A reliability test system for educational purposes-basic data,” *IEEE Transactions on Power Systems*, vol. 4, no. 3, pp. 1238–1244, Aug. 1989.

[22] ClusterTweed, “Roadmap h2 pour la wallonie,” https://fr.slideshare.net/cluster_tweed/roadmap-hydrogne-pour-la-wallonie-cluster-tweed, June 2018 (accessed 01/01/23).